Journal of Zhejiang University-SCIENCE B (Biomedicine & Biotechnology) 2021 22(7):575-589
www.jzus.zju.edu.cn; www.springer.com/journal/11585
E-mail: jzus_b@zju.edu.cn

Research Article
https://doi.org/10.1631/jzus.B2000520

Check for updates

Inhibitory mechanism of angiotensin-converting enzyme inhibitory peptides from black tea

Yating LU[1], Yu WANG[1], Danyi HUANG[1], Zhuang BIAN[1], Peng LU[2], Dongmei FAN[1], Xiaochang WANG[1]✉

[1]*Tea Research Institute, College of Agriculture and Biotechnology, Zhejiang University, Hangzhou 310058, China*
[2]*Department of Applied Biological Chemistry, Graduate School of Agricultural and Life Sciences, The University of Tokyo, Tokyo 113-8657, Japan*

Abstract: The aim of this work is to discover the inhibitory mechanism of tea peptides and to analyse the affinities between the peptides and the angiotensin-converting enzyme (ACE) as well as the stability of the complexes using in vitro and in silico methods. Four peptide sequences identified from tea, namely peptides I, II, III, and IV, were used to examine ACE inhibition and kinetics. The half maximal inhibitory concentration (IC_{50}) values of the four peptides were (210.03±18.29), (178.91±5.18), (196.31±2.87), and (121.11±3.38) μmol/L, respectively. The results of Lineweaver-Burk plots showed that peptides I, II, and IV inhibited ACE activity in an uncompetitive manner, which requires the presence of substrate. Peptide III inhibited ACE in a non-competitive manner, for which the presence of substrate is not necessary. The docking simulations showed that the four peptides did not bind to the active sites of ACE, indicating that the four peptides are allosteric inhibitors. The binding free energies calculated from molecular dynamic (MD) simulation were −72.47, −42.20, −52.10, and −67.14 kcal/mol (1 kcal=4.186 kJ), respectively. The lower IC_{50} value of peptide IV may be attributed to its stability when docking with ACE and changes in the flexibility and unfolding of ACE. These four bioactive peptides with ACE inhibitory ability can be incorporated into novel functional ingredients of black tea.

Key words: Black tea; Angiotensin-1-converting enzyme (ACE) inhibitory peptide; Kinetic study; Molecular docking; Molecular dynamic (MD) simulation

1 Introduction

Hypertension is the leading preventable cause of premature death worldwide because of its high prevalence and resulting complications (Mills et al., 2016). Long-term high blood pressure is normally considered a major risk factor for cardiovascular diseases (CVDs) such as atherosclerosis, coronary heart disease, stroke, and heart failure (Daskaya-Dikmen et al., 2017). It has been indicated that treatments that lower blood pressure can significantly reduce the risk of CVDs (Ettehad et al., 2016). Currently, angiotensin-converting enzyme (ACE; EC 3.4.15.1) is thought to perform a crucial function in controlling blood pressure (Hanif et al., 2010). ACE is a key component of the renin angiotensin system (RAS), an essential hormone system responsible for the homeostasis of blood pressure in mammals. It removes the C-terminal dipeptide from its substrate precursor peptide angiotensin I (AngI) to produce AngII, which is a potent vasoconstrictor and blocks the vasodilating properties of bradykinin, ultimately causing an increase in blood pressure (Harrison and Acharya, 2014). The first ACE inhibitors were found from the snake venom of *Bothrops jararaca* (Ferreira, 1965). Thereafter many synthetic ACE inhibitors, including captopril, enalapril, and lisinopril, were developed as effective antihypertensive drugs. However, they may cause certain adverse effects, including coughing, allergic reactions, taste disturbances, and skin rashes (Bougatef et al., 2008). People suffering from prehypertension (resting blood pressures between 120 mmHg/80 mmHg and 139 mmHg/89 mmHg (1 mmHg=0.133 kPa)) usually do not accept drug treatment because of the side effects and costs. However, lifestyle change including doing more exercise and taking healthy nutrients is urgently needed (Collier and Landram, 2012; Tao C et al., 2017). Thus, there

✉ Xiaochang WANG, xcwang@zju.edu.cn
Xiaochang WANG, https://orcid.org/0000-0002-9278-9867

Received Sept. 2, 2020; Revision accepted Feb. 21, 2021;
Crosschecked May 12, 2021

© Zhejiang University Press 2021

is a growing interest in discovering ACE inhibitors in natural products as alternatives or as co-adjuvant to synthetic drugs.

The identification of bioactive ACE inhibitory peptides derived from food proteins has become popular in recent years because of the excellent efficacy and safety of these peptides. They are inactive within the parent protein but exert positive physiological effects on systems of the body when released (Lafarga and Hayes, 2017). A large number of bioactive peptides have been isolated from bacteria, fungi, plants, animals, and even human bodies (Gu et al., 2011). The online database BIOPEP-UWM (http://www.uwm.edu.pl/biochemia) contains fundamental information about sequence databases and tools for the evaluation of proteins as the precursors of bioactive peptides. Over nine hundred bioactive peptides have been reported as ACE inhibitors in the BIOPEP database thus far. Most are from food sources, such as milk (Li et al., 2015), chicken muscle, tuna, soy, garlic, wheat, and olive seeds (Minkiewicz et al., 2008). Several studies have also reported in vivo ACE inhibitory activity of peptides (Escudero et al., 2013; Majumder et al., 2015). Therefore, ACE inhibitory peptides derived from food have received greater recognition and have been studied closely as potent natural and healthier alternatives to ACE inhibitor drugs.

More recently, in order to circumvent some challenges of the classical approach and interpret the mechanisms of action of novel ACE inhibitory peptides, in silico approaches have been widely used. For example, molecular docking has been applied to study the active mechanisms by which certain food-derived peptides inhibit ACE activity (Sornwatana et al., 2015). Molecular dynamic (MD) simulation has been used to further explore the interactions between inhibitors and receptors from a metabolic perspective (Guan et al., 2016).

Tea is a traditional health beverage in China, and its antioxidant (Satoh et al., 2005), antidiabetic (Wang et al., 2010; Zhang et al., 2010), and anti-hypertensive (Li et al., 2019) functions have been confirmed. In our previous studies, black tea was examined as a source of bioactive peptides for its special manufactory process such as fermentation, and four peptides (QTDEYGNPPR, AGFAGDDAPR, IDESLR, and IQDKEGIPPDQQR) with dipeptidyl-peptidase IV (DPP-IV) inhibitory activity were purified and identified using sodium dodecyl sulfate-polyacrylamide gel electrophoresis (SDS-PAGE) and liquid chromatography tandem mass spectrometer (LC-MS/MS) technologies (Lu et al., 2019). Certain peptides have been reported that are capable of exerting multiple types of physiological activity (Patil et al., 2015). For example, GYGGVSLPEW and LKPTPEGDLE derived from whey protein were reported as effective at inhibiting both ACE (half maximal inhibitory concentration (IC_{50}) =2 μmol/L) and DPP-IV (IC_{50}=42 μmol/L) (Lacroix et al., 2016). Diabetes and hypertension are believed to share a common pathway and a person with diabetes is more likely to suffer high blood pressure (Cheung and Li, 2012). Thus, in this study, we plan to investigate the ACE inhibitory activity of black tea peptides in vitro and to explore their inhibition patterns and mechanisms using the classic Lineweaver-Burk model as well as molecular docking/dynamic simulation. This study may provide a theoretical basis and experimental evidence for peptides in black tea as novel bioactive components and provide further evidence for black tea as a type of functional food.

2 Materials and methods

2.1 Materials

N-[3-(2-furyl)acryloyl]-L-phenylalanyl-glycyl-glycine (FAPGG; Lot: F7131), ACE (EC 3.4.15.1) from rabbit lung (Lot: A6778), and captopril (Lot: C8856) were purchased from Sigma-Aldrich (St. Louis, MO, USA). Black tea derived peptide sequences (QTDEYGNPPR, AGFAGDDAPR, IDESLR, and IQDKEGIPPDQQR) were synthesized by the Chinese Peptide Company (Hangzhou, China) with a purity of 96%–97%.

2.2 Assay for ACE inhibitory activity

ACE inhibitory activity was measured according to the method described by Shalaby et al. (2006) with minor modifications. Briefly, 10 μL of the ACE solution (final activity of 12.5 U/L) was mixed with 40 μL of the peptide solution (final concentrations were 100 to 700 μg/mL, dissolved in ultrapure water) in the wells of a 96-well microtiter plate at room temperature. Then, 150 μL of 0.88 mmol/L FAPGG (dissolved in 50 mmol/L Tris-HCl buffer containing 0.3 mol/L NaCl, pH 7.5, preheated at 37 °C, for 15 min) was added to each well in less than 1 min. Next, the microtiter plate

was immediately transferred to the microplate reader (Synergy H1, BioTek Instruments Inc., Vermont, USA). The rate of the decrease in absorbance at 345 nm was recorded for 30 min in 1-min intervals at 37 ℃. For control groups, 40 μL of buffer (50 mmol/L Tris-HCl buffer with 0.3 mol/L NaCl, pH 7.5) was used instead of the peptide solution. ACE activity was expressed as the slope of the decrease in absorbance (ρA), and the inhibitory activity was calculated according to the formula:

$$\text{ACE inhibition} = (1 - \rho A_{\text{inhibitor}}/\rho A_{\text{control}}) \times 100\%,$$

where $\rho A_{\text{inhibitor}}$ and ρA_{control} are the slopes obtained in the presence and absence of peptides, respectively. The IC_{50} values of tested samples were determined by the plot of ACE inhibition (%) against lg(sample concentration).

To determine the modes of ACE inhibition, the experiment was carried out with a set of concentrations of FAPGG substrate (0.88, 0.44, 0.22, and 0.11 mmol/L). V_0 is defined as the amount of FAPGG hydrolysed by ACE in 1 min at 37 ℃. The values of V_0 were measured in the absence and presence of peptide I (0.255 and 0.340 μmol/L), peptide II (0.205 and 0.307 μmol/L), peptide III (0.273 and 0.410 μmol/L), and peptide IV (0.273 and 0.410 μmol/L). The inhibition patterns of peptides were determined by Lineweaver-Burk plots. Non-competitive inhibitor, which does not necessarily need the presence of substrate, will change both the slope and the *y*-intercept. Uncompetitive inhibitor, which requires the presence of substrate, changes the *y*-intercept but not the slope. Competitive inhibitor changes the slope but not the *y*-intercept.

2.3 Molecular docking simulation

The structures of the peptides were obtained using the PEP-FOLD peptide structure prediction server (Shen et al., 2014). The crystal structures of ACE and captopril were obtained from the Research Collaboratory for Structural Bioinformatics Protein Data Bank (RCSB PDB; ACE was obtained from PDB structure 4APH and captopril was obtained from PDB structure 1UZF). The structure of FAPGG was obtained from the PubChem database. The structure removing glycyl-glycine (GG) from FAPGG was used as the structure of *N*-[3-(2-furyl)acryloyl]-L-phenylalanyl (FAP). The ACE protein was prepared by removing water molecules and co-crystal ligands. Molecular docking was performed using AutoDock Vina Version 1.1.2 (Trott and Olson, 2010), A grid of 40×40×40 points in the *x*-, *y*-, and *z*-axis directions was built with a grid spacing of 1 Å. Docking FAPGG to ACE was performed before the docking of peptides I, II, and IV because they were uncompetitive inhibitors. The mode with the lowest affinity value was chosen as the final docking result.

2.4 Molecular dynamic simulation

All the complex systems were subjected to MD simulation using the Amber 17 project (Case et al., 2005). Each complex was solvated in an octahedral box full of TIP3P water molecules. Sodium ions were placed to keep the whole system neutral and at minimum energy. The leaprc.protein.ff14SB force field was used to perform the 100 ns MD simulation. The coordinate bonds between Zn (II) and its surroundings were treated by the Metal Center Parameter Builder (MCPB) method (Yu et al., 2019). The MD simulations at 300 K were performed for 100 ns, and the MD time step was taken as 0.02 s; thus 5000 conformations were obtained in each MD simulation.

2.5 Binding free energy and ligand–residue interaction decomposition calculation

After simulation, the binding free energies were calculated using the molecular mechanics/Poisson-Boltzmann surface area (MM-PBSA) approach in Amber 17. This is suitable for various molecular systems. The concepts and the practical procedures of this approach have been described in detail elsewhere (Homeyer and Gohlke, 2012). A total of 100 snapshots were extracted from the 5000 MD trajectories (100 ns) equably for calculation, and the interval was 50 trajectories. The interactions between each ligand (peptide) and every residue in the ACE protein were analysed using the MM-PBSA decomposition process applied in the MM-PBSA module in Amber 17. The snapshots extracted from this procedure were the same as those in the binding free energy calculations.

2.6 Statistical analysis

The assays of ACE inhibitory activity were carried out with three replications and data were presented as mean±standard deviation (SD). Significant differences of ACE inhibitory activity were analysed using Ryan-Einot-Gabriel-Welsch multiple range (REGWQ) test (P<0.05) in Statistical Analysis System (SAS) University Edition (Institute Inc., Cary, NC, USA).

3 Results

3.1 ACE inhibitory activity of tea peptides

Four synthetic peptides identified in black tea were tested for ACE inhibitory activity at concentrations ranging from 100 to 700 μg/mL. The unit of concentration was converted to μmol/L according to the peptide molecular weights. The IC_{50} values for four peptides are presented in Table 1. Tridecapeptide IQDKEGIPPDQQR (peptide IV) exhibited the strongest inhibitory capacity with the lowest IC_{50} value of (121.11±3.38) μmol/L, compared to AGFAGDDAPR (peptide II, (178.91±5.18) μmol/L), the hexapeptide IDESLR (peptide III, (196.31±2.87) μmol/L), and decapeptide QTDEYGNPPR (peptide I, (210.03±18.29) μmol/L). The IC_{50} value of captopril (positive control) was (21.78±1.10) nmol/L, which was consistent with the IC_{50} range obtained by others (7–22 nmol/L) (Shalaby et al., 2006).

3.2 Kinetics of ACE inhibition activity

The ACE inhibition patterns of the four peptides were evaluated by Lineweaver-Burk plots. The regression curves of different peptide concentrations were parallel for peptides I, II, and IV, exhibiting uncompetitive inhibition (Figs. 1a, 1b, and 1d). The regression curves of different concentrations of peptide III intersected at the 1/[*S*] axis, indicating that the inhibition was non-competitive (Fig. 1c).

3.3 Molecular docking of tea peptides and ACE

The different IC_{50} values and inhibition patterns among the four peptides indicated that these peptides inhibit ACE through different mechanisms. Therefore,

Table 1 Molecular weight, half maximal inhibitory concentration (IC_{50}) values, and binding free energy of four peptides

Sample	Peptide sequence	Molecular mass (Da)	IC_{50}	Binding free energy (kcal/mol)
Peptide I	QTDEYGNPPR	1176	(210.03±18.29)^{a} μmol/L	−72.47
Peptide II	AGFAGDDAPR	976	(178.91±5.18)^{b} μmol/L	−42.20
Peptide III	IDESLR	731	(196.31±2.87)^{ab} μmol/L	−52.10
Peptide IV	IQDKEGIPPDQQR	1523	(121.11±3.38)^{c} μmol/L	−67.14
Captopril		217	(21.78±1.10) nmol/L	−24.20

The IC_{50} values are expressed as mean±standard deviation (SD), n=3. Means with the same letters (a, b, c) are not significantly different (P> 0.05). 1 kcal=4.186 kJ.

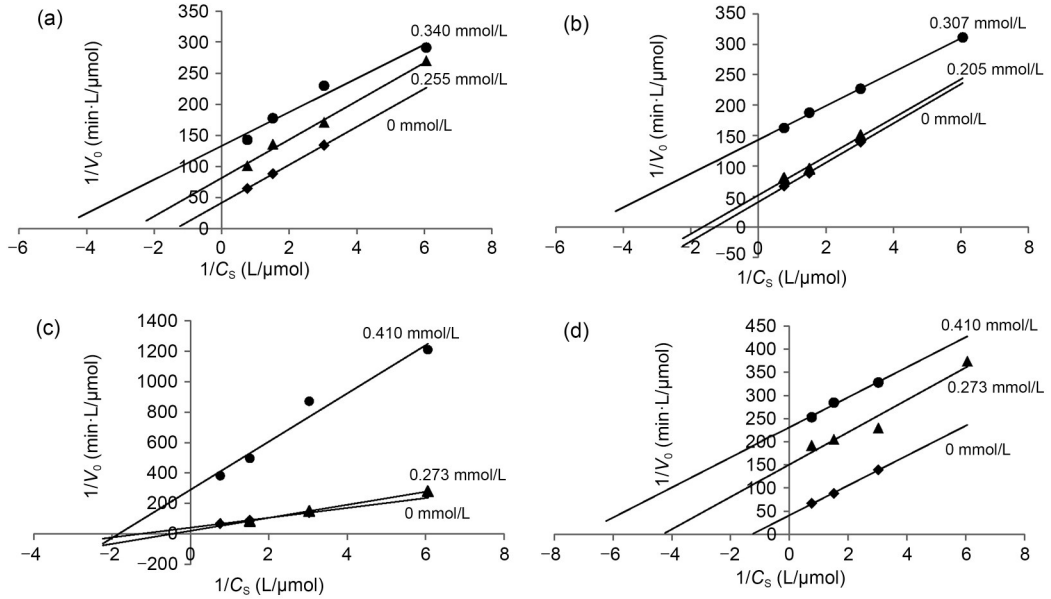

Fig. 1 Angiotensin-converting enzyme (ACE) inhibition patterns of peptides I, II, III, and IV at different concentrations were determined using Lineweaver-Burk plots. V_0 is defined as the amount of FAPGG hydrolysed by ACE in 1 min at 37°, and C_S means the concentration of FAPGG substrate. (a) Peptide I, uncompetitive inhibition pattern; (b) Peptide II, uncompetitive inhibition pattern; (c) Peptide III, non-competitive inhibition pattern; (d) Peptide IV, uncompetitive inhibition pattern.

molecular docking was performed to further investigate the interactions and to predict the preferred orientations of these four peptides when they bind to ACE. The best docking modes with the lowest affinity values are shown in Fig. 2. Peptides I, II, III, and IV were all located in a long cleft in ACE away from the active pockets. The interactions of ACE with four peptide ligands were detected and plotted using the LigPlot+ program (Laskowski and Swindells, 2011). The results presented in Fig. 3 show that interactions including hydrogen bonds, hydrophobic forces, and van der Waals contacts can be observed. Fifteen hydrogen bonds were formed between amino acids of peptide I and residues of ACE (Fig. 3a). Six hydrogen bonds were found between amino acids of peptide II and residues of ACE in Fig. 3b. Only two hydrogen bonds were formed between peptide III and ACE (Fig. 3c), while peptide IV was surrounded by an extensive network of interactive residues from ACE (Fig. 3d). The carbonyl oxygen atoms and amidogen hydrogen atoms of $Gln2^{IV}$ contributed four hydrogen bonds, $Ile1^{IV}$, $Pro9^{IV}$, and $Asp10^{IV}$ contributed two hydrogen bonds each. $Lys4^{IV}$ and $Arg13^{IV}$ were stabilized with residues $Thr92^{ACE}$ and $Lys118^{ACE}$ by one hydrogen bond interaction. On the other sides, captopril was docked in the cavity near the active pockets and formed hydrogen bonds with $Tyr520^{ACE}$ and $Gln281^{ACE}$ (Fig. 2).

3.4 Molecular dynamic simulation of tea peptides and ACE

The conformations selected from molecular docking were performed with dynamic simulation to further validate their interaction mechanisms. Total binding free energies and contributions of residues surrounding peptides were calculated by the MM-PBSA approach. The binding free energy of peptide I was the lowest (−72.47 kcal/mol, 1 kcal=4.186 kJ), followed by peptide IV (−67.14 kcal/mol) and peptide III (−52.10 kcal/mol), and the value of peptide II was the highest (−42.20 kcal/mol) (Table 1).

The van der Waals (ΔE_{vdw}), electrostatic (ΔE_{ele}), polar solvation (ΔE_{sol}), and total (ΔE_{total}) contributions of the residues to the binding free energy of the ACE–peptide complex were also calculated by the MM-PBSA method. Electrostatic interactions play an important part in the formation of hydrogen bonds; in the presence of strong electrostatic interactions, several hydrogen bonds can easily form (Guan et al., 2016). $Arg124^{ACE}$ contributes the most electrostatic energy to the peptide I–ACE complex (Fig. 4a). $Trp59^{ACE}$ and

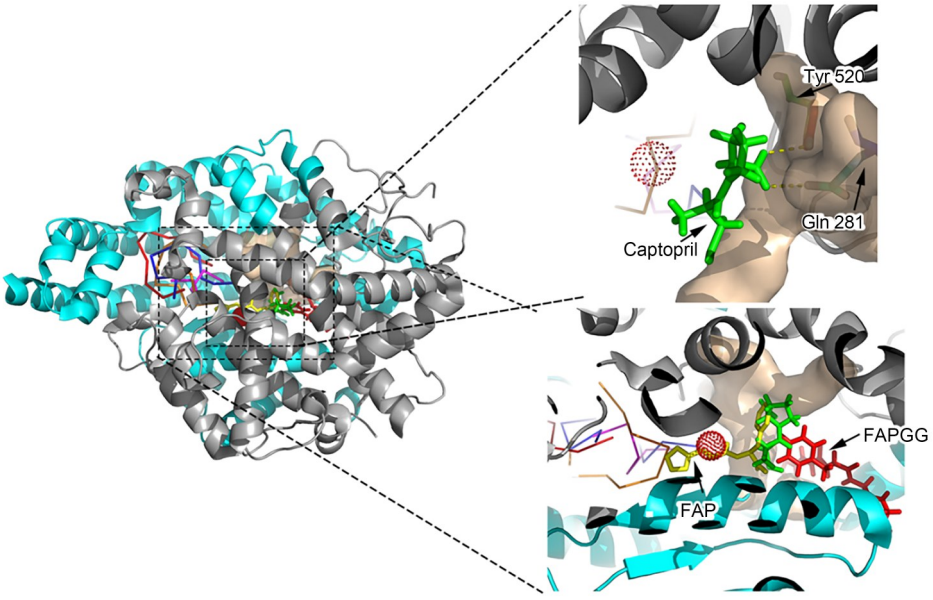

Fig. 2 Binding sites of peptides I, II, III, IV, captopril, *N*-[3-(2-furyl)acryloyl]-L-phenylalanyl-glycyl-glycine (FAPGG), and *N*-[3-(2-furyl)acryloyl]-L-phenylalanyl (FAP) within the structure of angiotensin-converting enzyme (ACE). Peptides I, II, III, and IV are shown as ribbons colored in blue, red, magenta, and orange, respectively. FAPGG, FAP, and captopril are shown as sticks colored in red, yellow, and green, respectively. The ACE enzyme is shown as a cartoon in grey and cyan according to the root mean square fluctuation (RMSF) value. Zn (II) in ACE is shown as a red dot. The active pockets of ACE are colored in wheat.

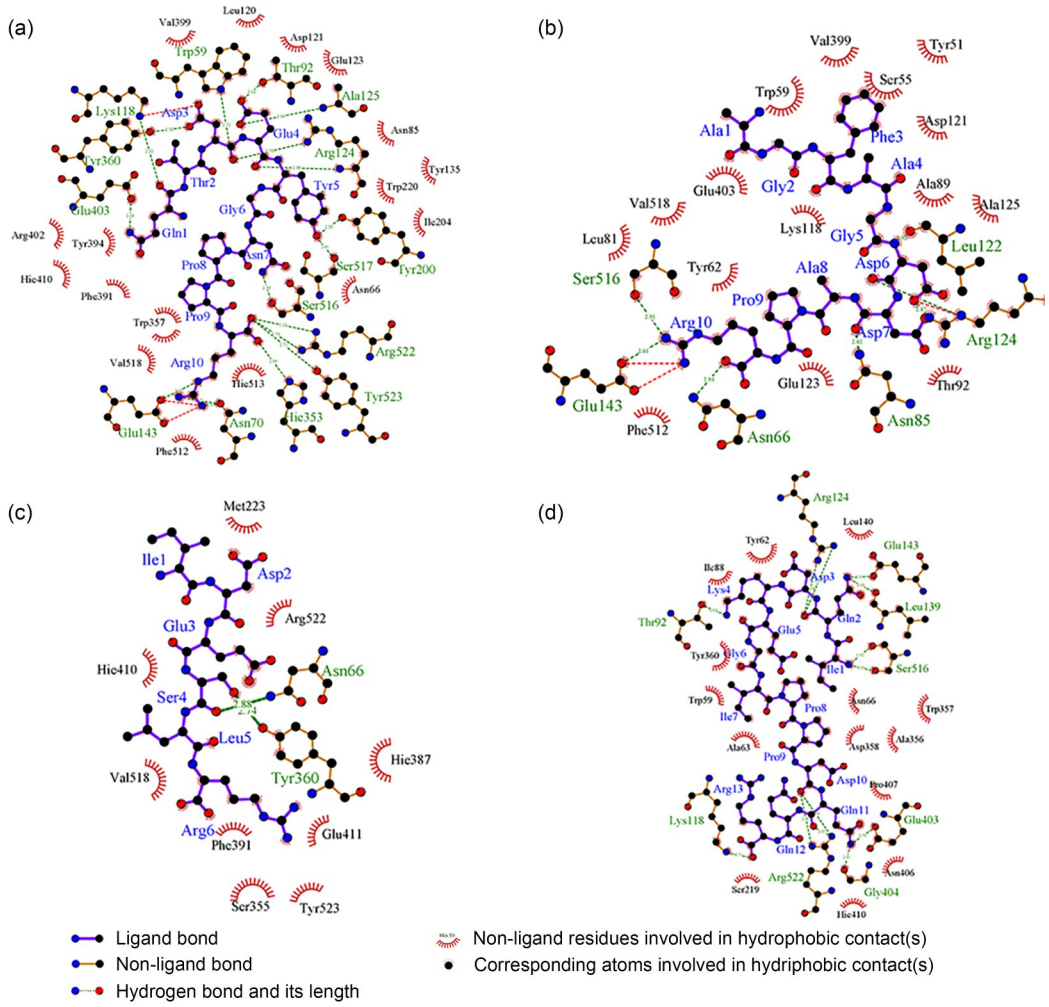

Fig. 3 Schematic representation of interactions across the interfaces of peptide–angiotensin-converting enzyme (ACE) complexes generated using LigPlot+. (a) Peptide I–ACE complex; (b) Peptide II–ACE complex; (c) Peptide III–ACE complex; (d) Peptide IV–ACE complex.

Arg124^{ACE} both contributed remarkable total energy to the combinations of peptide II–ACE (Fig. 4b). Arg124^{ACE}, Lys368^{ACE}, and Arg522^{ACE} all contributed both electrostatic and total energies (Fig. 4c). Trp59^{ACE}, Tyr62^{ACE}, Glu143^{ACE}, Trp357^{ACE}, and Ser516^{ACE} show clear total energy values in Fig. 4d. In addition, Lys118^{ACE}, Asp121^{ACE}, and Arg522^{ACE} make significant electrostatic contributions.

The initial binding orientations of peptides may change at different phases during simulation. Thus, the numbers of hydrogen bonds between ACE and inhibitory peptides were further confirmed by the results of MD simulations (Fig. 5). Peptide I can form more hydrogen bonds with ACE than can the other three peptides. Over ten hydrogen bonds can be constantly observed during the entire MD process, and the maximum number of hydrogen bonds formed was 25. The number of hydrogen bonds with ACE of peptide IV was fewer than that of peptide I but more than those of peptides II and III. The probabilities and details of occurrence of hydrogen bonds are shown in Table 2. Peptide I can form hydrogen bonds with 19 residues of ACE. Peptide II can form hydrogen bonds with 15 residues of ACE. However, the most presence of hydrogen bonds during MD simulation between peptide II and ACE was only 45.56%. Ser355^{ACE}, Arg522^{ACE}, Asn66^{ACE}, Trp357^{ACE}, Arg124^{ACE}, Glu384^{ACE}, Lys368^{ACE}, Glu403^{ACE}, and Hie513^{ACE} might form hydrogen bonds with peptide III. Peptide IV has a probability of occurrence of hydrogen bonding with 14 residues of ACE,

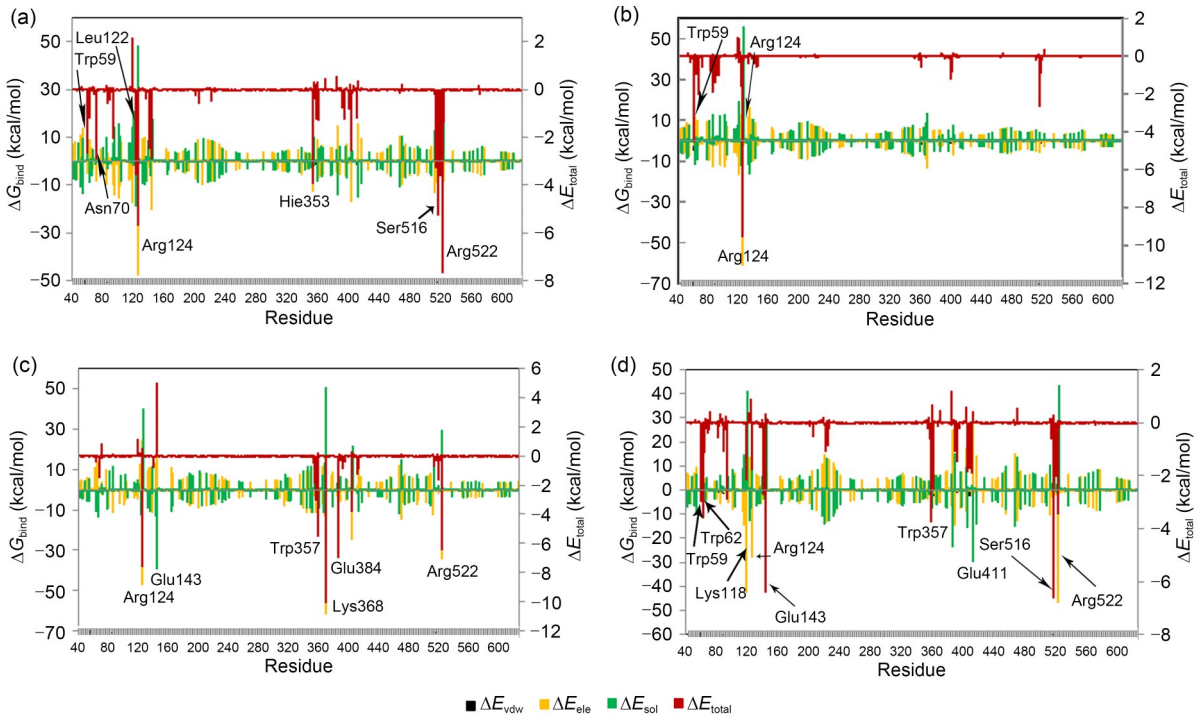

Fig. 4 Decomposition of binding energy per residue based on peptide I – angiotensin-converting enzyme (ACE) (a), peptide II–ACE (b), peptide III–ACE (c), and peptide IV–ACE (d). ΔE_{vdw}: van der Waals contribution to the binding free energy; ΔE_{ele}: electrostatic contribution to the binding free energy; ΔE_{sol}: polar solvation contribution to the binding free energy; ΔE_{total}: total contribution to the binding free energy; ΔG_{bind}: binding energy.

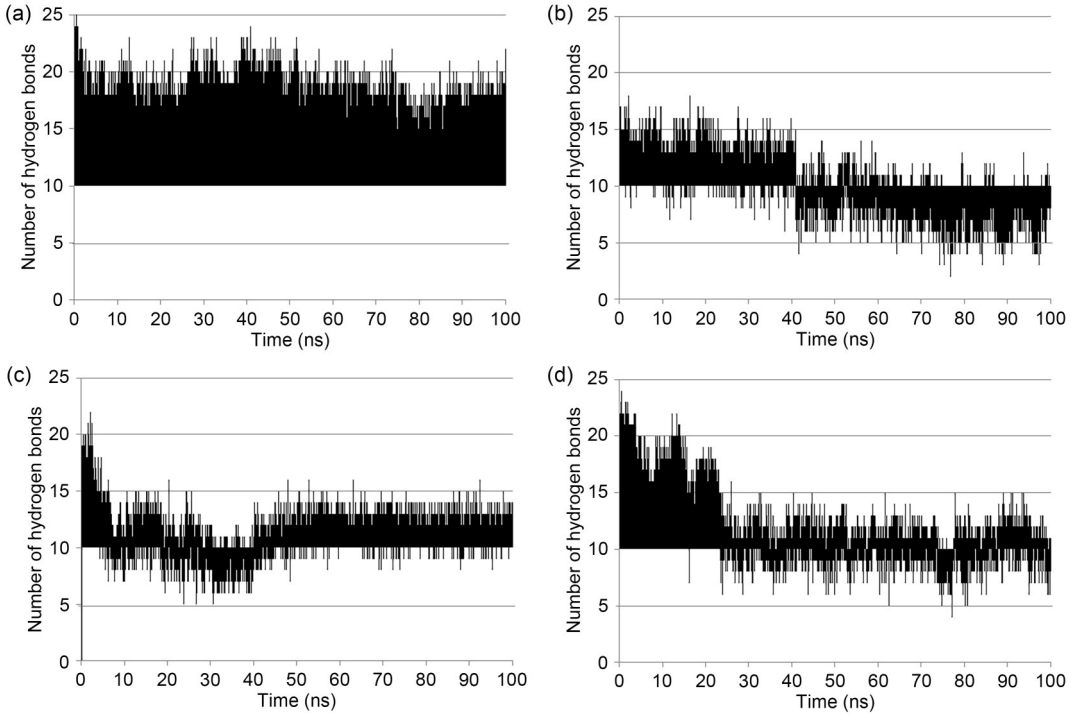

Fig. 5 Numbers of hydrogen bonds between angiotensin-converting enzyme (ACE) and peptides during molecular dynamic (MD) simulation: (a) peptide I; (b) peptide II; (c) peptide III; and (d) peptide IV. The line of 10 hydrogen bonds was set as the reference line.

Table 2 Hydrogen bond occupancies for ACE–peptide complexes

Acceptor	Donor	Presence (%)	Acceptor	Donor	Presence (%)
Peptide I			Glu4^{I}OE2	Ala125N	7.68
Arg10^{I}O	Arg522NH2	86.32	Arg10^{I}OXT	Tyr523OH	7.54
Glu4^{I}OE1	Arg124NH2	69.46	Asp3^{I}O	Arg124NH2	5.42
Arg10^{I}O	Arg522NH1	68.30	Peptide II		
Asn70OD1	Arg10^{I}NH2	64.40	Asp6^{II}OD2	Arg124NH2	45.56
Ser517O	Tyr5^{I}OH	59.00	Asp7^{II}O	Asn85ND2	40.08
Asp3^{I}OD2	Tyr360OH	56.28	Glu403OE2	Phe3^{II}N	38.82
Ser516OG	Arg10^{I}NE	54.20	Glu403OE1	Gly2^{II}N	38.06
Glu143OE1	Arg10^{I}NH2	46.94	Asp6^{II}O	Arg124NE	33.52
Tyr5^{I}O	TyR62OH	46.22	Leu122O	Asp6^{II}N	29.72
Arg10^{I}O	Tyr523OH	44.92	Asp6^{II}HB3	Ala125N	27.26
Glu4^{I}OE1	Arg124NE	44.48	Ser516O	Arg10^{II}NH1	23.72
Glu143OE2	Arg10^{I}NH2	44.38	Asp7^{II}OD1	Tyr62OH	21.66
Asn70OD1	Arg10^{I}NH1	42.02	Arg10^{II}O	Asn66ND2	18.64
Glu4^{I}OE2	Thr92OG1	41.38	Arg10^{II}OXT	Ser355OG	18.62
Asp3^{I}OD1	Tyr360OH	41.04	Asp6^{II}OD2	Asn85ND2	18.06
Arg10^{I}OXT	Hie353NE2	40.16	Asp7^{II}O	Arg124NH1	17.56
Ser517OG	Tyr5^{I}OH	29.20	Arg10^{II}O	Trp357NE1	17.06
Ser516HG	Arg10^{I}NE	27.28	Arg10^{II}OXT	Asn66ND2	16.64
Asn7^{I}OD1	Ser517OG	25.54	Asp7^{II}O	Arg124NH2	16.42
Glu4^{I}OE1	Thr92OG1	25.06	Glu403OE2	Gly2^{II}N	14.76
Glu4^{I}OE2	Arg124NE	24.94	Asp6^{II}OD1	Arg124NH2	14.24
Leu139O	Asn7^{I}ND2	24.00	Arg10^{II}OXT	Trp357NE1	13.84
Arg402O	Gln1^{I}N	22.34	Asp358OD1	Ala1^{II}N	13.14
Arg402O	Gln1^{I}N	22.00	Gly2^{II}O	Tyr360OH	13.12
Glu143OE1	Asn7^{I}ND2	21.64	Arg10^{II}O	Ser355OG	12.90
Tyr5^{I}OH	Tyr200OH	21.02	Asp6^{II}O	Arg124N	12.88
Arg402O	Gln1^{I}N	20.70	Ala1^{II}O	Tyr360OH	12.78
Glu143OE2	Asn7^{I}ND2	19.84	Asp358OD1	Ala1^{II}N	12.54
Arg10^{I}OXT	Hie513NE2	18.60	Asp358OD1	Ala1^{II}N	12.42
Ser516OG	Asn7^{I}ND2	18.30	Phe3^{II}O	Lys118NZ	11.22
Asp3^{I}O	Trp59NE1	15.92	Phe3^{II}O	Lys118NZ	10.04
Glu403OE1	Gln1^{I}N	15.02	Phe3^{II}O	Lys118NZ	10.04
Glu403OE1	Gln1^{I}N	14.76	Arg402O	Ala1^{II}N	7.34
Glu403OE1	Gln1^{I}N	13.34	Arg10^{II}OXT	Lys368NZ	6.90
Asp3^{I}OD1	Lys118NZ	13.02	Arg402O	Ala1^{II}N	6.80
Asp3^{I}OD1	Lys118NZ	10.20	Arg10^{II}O	Asn70ND2	6.76
Asp3^{I}OD1	Lys118NZ	9.82	Arg10^{II}OXT	Lys368NZ	6.48
Tyr62OH	Thr2^{I}OG1	9.72	Arg402O	Ala1^{II}N	6.44

To be continued

Table 2

Acceptor	Donor	Presence (%)	Acceptor	Donor	Presence (%)
Arg10^{II}OXT	Lys368NZ	5.82	Gln2^{IV}O	Arg124NH1	38.26
Ser516O	Arg10^{II}NH2	5.62	Glu123OE1	Arg13^{IV}NH2	34.76
Arg10^{II}O	Lys368NZ	5.06	Glu143OE1	Gln2^{IV}NE2	31.94
Peptide III			Glu123OE2	Arg13^{IV}NH2	31.10
Arg6^{III}O	Ser355OG	98.94	Glu403OE2	Gln11^{IV}NE2	29.98
Glu3^{III}OE2	Arg522NH1	65.20	Glu143OE2	Gln2^{IV}NE2	29.04
Ser4^{III}O	Asn66ND2	62.36	Asp3^{IV}O	Arg124NH1	25.42
Arg6^{III}O	Trp357NE1	59.90	Asp10^{IV}OD1	Arg522NH2	17.86
Glu3^{III}OE1	Arg522NH2	59.24	Glu143OE1	Ile1^{IV}N	17.16
Asp2^{III}OD2	Arg124NH2	58.94	Asp10^{IV}OD1	Arg522NH1	17.14
Glu384OE2	Arg6^{III}NH2	39.58	Glu143OE2	Ile1^{IV}N	15.98
Arg6^{III}O	Lys368NZ	28.68	Glu143OE1	Ile1^{IV}N	15.96
Glu384OE1	Arg6^{III}NH2	49.50	Glu143OE1	Ile1^{IV}N	15.52
Asp2^{III}OD1	Arg124NH1	45.90	Glu403OE1	Gln11^{IV}NE2	15.20
Glu384OE2	Arg6^{III}NH1	42.26	Glu143OE2	Ile1^{IV}N	15.08
Glu384OE1	Arg6^{III}NH1	42.20	Gln11^{IV}O	Arg522NH2	15.04
Glu403OE2	Ile1^{III}N	15.04	Asn66OD1	Gln2^{IV}NE2	14.64
Glu403OE1	Ile1^{III}N	14.20	Asp10^{IV}OD2	Ser355OG	13.94
Asp2^{III}OD2	Arg124NH1	9.02	Gln11^{IV}OE1	Gly404N	11.64
Arg6^{III}OXT	Lys368NZ	7.02	Asp3^{IV}OD2	Tyr135OH	11.34
Arg6^{III}O	Lys368NZ	28.46	Glu143OE2	Ile1^{IV}N	10.88
Arg6^{III}O	Lys368NZ	22.70	Arg13^{IV}O	Lys118NZ	9.88
Glu3^{III}OE1	Arg522NH1	19.96	Asp10^{IV}O	Arg522NH2	9.68
Glu403OE1	Ile1^{III}N	15.08	Gln2^{IV}OE1	Tyr62OH	9.28
Arg6^{III}OXT	Lys368NZ	6.94	Arg13^{IV}O	Lys118NZ	7.88
Leu5^{III}O	Hie513NE2	6.40	Glu123OE1	Lys4^{IV}NZ	7.84
Arg6^{III}OXT	Lys368NZ	6.06	Gly6^{IV}O	Tyr360OH	7.68
Arg6^{III}OXT	Hie513NE2	5.78	Arg13^{IV}O	Lys118NZ	7.60
Glu403OE1	Ile1^{III}N	13.70	Glu123OE2	Arg13^{IV}NH1	7.60
Glu403OE2	Ile1^{III}N	12.44	Ser516O	Ile1^{IV}N	7.22
Glu403OE2	Ile1^{III}N	11.04	Ser516O	Ile1^{IV}N	7.18
Glu3^{III}OE2	Arg522NH2	9.78	Arg13^{IV}OXT	Lys118NZ	6.78
Asp2^{III}OD1	Arg124NH2	5.66	Ala356O	Asp10^{IV}N	6.72
Peptide IV			Ser516O	Ile1^{IV}N	6.68
Asp10^{IV}O	Arg522NH1	71.60	Ser516OG	Ile1^{IV}N	6.08
Gln2^{IV}O	Arg124NH2	67.92	Arg13^{IV}OXT	Lys118NZ	5.90
Gly404O	Gln11^{IV}NE2	60.88	Arg13^{IV}OXT	Lys118NZ	5.80
Gln11^{IV}O	Arg522NH2	58.74	Leu139O	Gln2^{IV}NE2	5.64
Gln2^{IV}OE1	Asn85ND2	47.36	Asn66OD1	Gln2^{IV}N	5.32

including Asn66^{ACE}, Asn85^{ACE}, Lys118^{ACE}, Glu123^{ACE}, Arg124^{ACE}, Tyr135^{ACE}, Leu139^{ACE}, Glu143^{ACE}, Ser355^{ACE}, Ala356^{ACE}, Glu403^{ACE}, Gly404^{ACE}, Ser516^{ACE}, and Arg522^{ACE}.

The stability of the ACE protein/peptide complexes during their binding processes was predicted using root mean square deviation (RMSD) analysis. Five thousand trajectories obtained from the 100-ns dynamic simulation were used in this analysis. The RMSD of ACE increased after inhibitors (peptides and captopril) bound to it (Fig. 6a). However, the RMSD of ACE combined with captopril rose and fluctuated very slightly. The RMSD of ACE combined with peptide IV increased to a higher level than that with captopril but lower than those with the other three peptides. The fluctuation of RMSD of peptide IV was most stable of the four peptides when coupled to ACE (Fig. 6b). Generally, the radius of gyration (R_g) was used to describe the degree of unfolding of a protein to its native state (Wang et al., 2016). The variations in R_g indicated that all four peptides and the captopril were able to loosen ACE after binding. The tightness of ACE changed least after binding with peptide I. Peptide II had the strongest effect on the unfolding of ACE and peptide IV had a similar effect with captopril (Fig. 6c). The average distance between the C-terminal carboxylic oxygen of each peptide and the zinc atom is shown in Fig. 6d. When the system of the dynamics process reached balance after 60 ns, the distance between the C-terminal carboxylic oxygen of peptide IV and the zinc atom was the longest of the four peptides followed by peptides II, III, and I in sequence. The root mean square fluctuation (RMSF) values reflect the fluctuations of individual residues; a lower RMSF value indicates greater stability (Ning et al., 2018). Both peptides and captopril can make ACE more flexible (Fig. 7). After binding, in regions 40–204,

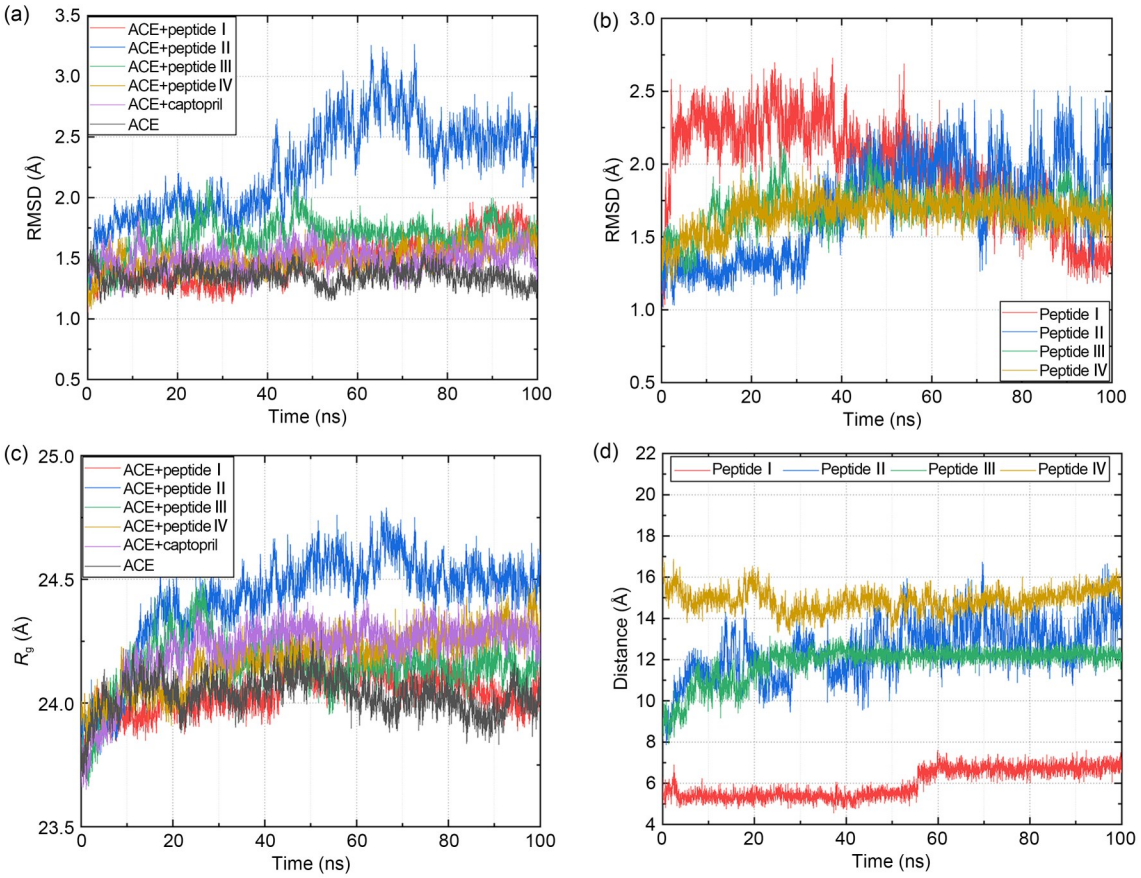

Fig. 6 Stability of peptides–angiotensin-converting enzyme (ACE) complex and the influence of peptides on ACE. (a) Root mean square deviation (RMSD) of ACE with and without peptides and captopril. (b) RMSD of peptides docked into ACE. (c) Radius of gyration (R_g) of ACE with and without inhibitors (peptides and captopril). (d) Average distance between the C-terminal carboxylic oxygen of each peptide and the zinc atom of ACE. RMSD, R_g, and distance in angstroms (1 Å=10^{-10} m) are plotted versus time. Molecular dynamic (MD) simulation was performed over 100 ns.

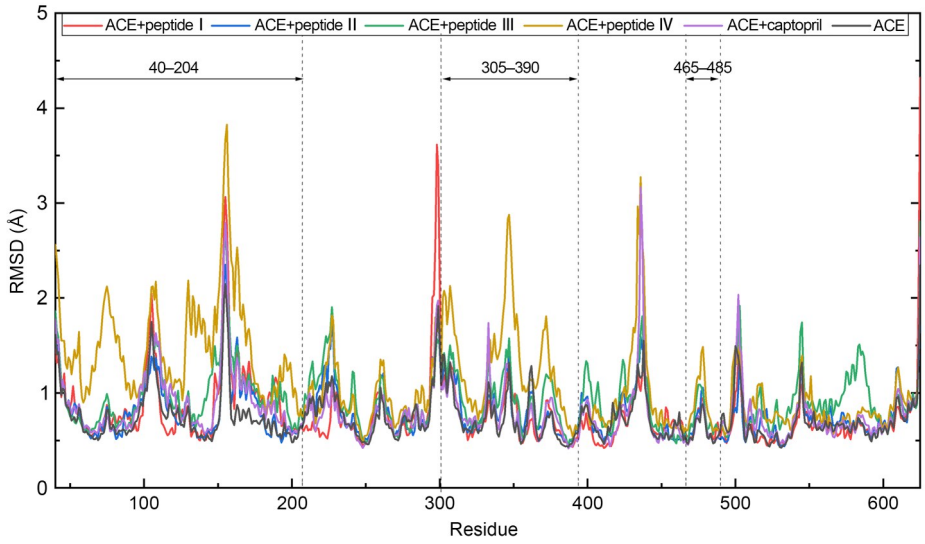

Fig. 7 Root mean square fluctuation (RMSF) of angiotensin-converting enzyme (ACE) with and without inhibitors (peptides and captopril) during molecular dynamic (MD) simulation.

305–390, 465–485, captopril does not significantly change the RMSF value of ACE, but the value is evidently increased by four peptides at different time (Figs. 2 and 7).

4 Discussion

Food-derived ACE inhibitory peptides are diverse in source, sequence length, amino acid constitution, and IC_{50} values. Studies of the structure–activity relationship of ACE inhibitory peptides showed the presence of tyrosine (Y), phenylalanine (F), tryptophan (W), proline (P), lysine (K), isoleucine (I), valine (V), leucine (L), and arginine (R) in the peptides and amino acids with positive charges at the C-terminus exerting a strong influence on ACE binding (Daskaya-Dikmen et al., 2017). Kumar et al. (2015) identified 1745 antihypertensive peptides (AHTPs) from the literature and publicly available datasets and obtained random fragments from the Swiss-Prot proteins as a negative database to build a platform for predicting, screening, and designing AHTPs. They reported that residue P is highly abundant in AHTPs but amino acids such as aspartic acid (D) and serine (S) are less frequent in most AHTPs in comparison to non-AHTPs. In our study, peptides I, II, and IV all include P in their sequences, which may help to improve their inhibitory capacity. On the other hand, peptide III does not contain P but includes both D and S in its sequence, which may weaken its inhibitory potency. Using Kumar's platform (Kumar et al., 2015), the four peptides in our study obtained scores of 0.12, 0.24, −1.07, and 1.00, respectively. These results were consistent with their IC_{50} values obtained from the in vitro experiments. Thus, amino acid composition could have an important effect on antihypertensive potency. Moreover, judging from hydrogen bond occupancies for ACE–peptide complexes during the MD process, R of the four peptides all contribute most to the formation of hydrogen bonds for the stabilization of the complex (Table 2). This indicates that R is of great importance in the inhibition of ACE.

Most food-derived peptides inhibit ACE in a competitive or non-competitive manner (Puchalska et al., 2015). The peptides with competitive inhibition mode usually bind with the active site of ACE via hydrogen bonds (Chamata et al., 2020; Zheng et al., 2020), and even coordinate with Zn (II) of ACE (Tao ML et al., 2017). ACE has three main active site pockets: S1, S2, and S1'. S1 pocket includes Ala354, Glu384, and Tyr523 residues; S2 pocket includes Gln281, His353, Lys511, His513, and Tyr520 residues; and S1' includes Glu162 residue (Zheng et al., 2019). The result of molecular docking of captopril (a competitive positive control) in our study showed that captopril binds to the S2 pocket and forms hydrogen bonds with Tyr520 and Gln281. Peptides with a non-competitive inhibition pattern can work with or without the substrate present. Although it has been reported that a non-competitive

inhibitory peptide YLVR could bind with certain amino acids in the ACE active site through cation–pi interactions (Liu et al., 2018), they usually cannot form hydrogen bonds with crucial amino acid residues in the active site of ACE (Zhao et al., 2019). As in our study, peptide III acted as a non-competitive inhibitor that does not bind the active sites of ACE. Peptides with competitive inhibition mode can have interactions with the active site pockets of ACE, but this does not mean that they certainly have better inhibitory activity. For example, ASL (IC_{50}=102.15 μmol/L), AFKDETEEVPFR (IC_{50}=80.20 μmol/L), and CRQNTLGHNTQTSIAQ (IC_{50}=80.00 μmol/L) present competitive, non-competitive, and uncompetitive inhibition patterns, respectively. Among these three peptides, the competitive inhibitory peptide (ASL) does not show stronger inhibitory activity than the others (Tanzadehpanah et al., 2013; Wu et al., 2015; Forghani et al., 2016). Therefore, the ACE inhibitory potency of peptides in different inhibition modes cannot be directly compared.

As far as we know, only a few peptides are reported to exhibit uncompetitive inhibition, in which the peptide only binds to the enzyme–substrate complex and the inhibitor does not compete with the substrate, such as CRQNTLGHNTQTSIAQ from *Stichopus horrens* (Forghani et al., 2016) and FESNFNTQATNR from lysozyme hydrolysate (Asoodeh et al., 2012). Thus, the inhibition mechanism of uncompetitive inhibitory peptides has not been clearly illustrated. In our research, interestingly, peptides I, II, and IV all showed an uncompetitive mode of inhibition. The in vitro ACE inhibitory activity of peptide IV was higher than that of peptides II and I. The RMSD value of peptide IV was the lowest, which means that the stability of peptide IV was the highest, although the hydrogen bond number between ACE and peptide I was higher than that of peptide IV during MD simulation. In addition, the RMSF of ACE was enhanced most by peptide IV. The R_g of peptide IV was higher than that of peptide I, which means peptide IV could significantly change the structure of ACE. Thus, our peptides may inhibit the activity of ACE by changing its conformation. After FAPGG (the ACE substrate) binds to ACE, it is hydrolysed to FAP. Our black tea peptides are located at the exit channel of the cavity where FAP is docked (Fig. 2). Our peptides with uncompetitive inhibitory mode may also block the dissociation of hydrolysis product of the substrate, and finally the hydrolysis will also act as an inhibitor of ACE. The inhibitory peptides with the same inhibiton mode could be affected by the distance between the C-terminal carboxylic oxygen of peptide and the zinc atom of ACE (Gunalan et al., 2020). In our study, results of MD simulation showed that the distance between peptide IV and the zinc atom of ACE is longer than those of peptides II and I.

In vitro inhibitory activity is a requirement for natural peptides to be a blood pressure-lowering material, and the in vivo biostability and bioavailability of peptides must also be considered. First of all, peptides should remain stable against gastrointestinal enzymes, because oral administration is considered to be the main intake route. Peptides could be digested by internal proteases in vivo and consequently alter their ACE inhibitory activity, compared to the ACE inhibitory activity of the peptides in vitro. For example, the ACE inhibitory activity of the peptide LVLPGELAK is enhanced twofold after simulated digestion, compared to the original value as in vitro (Dang et al., 2019). However, peptide YGGY (IC_{50}=3.4 μmol/L) loses its inhibitory activity after simulated digestion (Saito et al., 1994). Some peptides could retain their activity after gastrointestinal enzyme digestion peptides such as RGQVIYVL, ASPKPSSA, and QFLLAGR isolated from quinoa branalbumin (Zheng et al., 2019) and SSYYPFK isolated from naked oat globulin (Zheng et al., 2020). It has been mentioned that the sequence and position of the amino acids of peptides determine their ability against gastrointestinal enzymes (Martin and Deussen, 2019). Sharma et al. (2014) developed a web sever "HLP" (http://crdd.osdd.net/raghava/hlp) to predict the half-life of peptides in an intestine-like environment and it can be used to predict the susceptibility of peptides towards protease degradation. The results analyzed by this server showed that peptides II, III, and IV presented high stability and peptide I presented normal stability. We noticed that peptide IV may be a substrate of trypsin. However, peptides containing Lys resisting gastrointestinal digestion have been reported both in vitro and in vivo (García-Mora et al., 2017; Fan et al., 2019).

First, the small intestinal epithelium plays a crucial role in the absorption of nutrients and it is also a barrier against unfavourable substances in food. Second, peptides should be efficiently absorbed by the intestinal epithelium. Di- and tri-peptides are mainly transported via specific oligopeptide transporter proteins (peptide-transporters 1 (PEPT1)) of the absorptive cells (Shimizu, 1999; Groneberg et al., 2001). Paracellular pathways and transcytosis can help oligopeptides, with amino acid residues ranging from three to more, to transport

(Miner-Williams et al., 2014). For example, the Caco-2 cell monolayer model is often used in simulated intestinal transport experiments in vitro. QIGLF (IC_{50}= 75.00 μmol/L) derived from egg white ovalbumin can be absorbed intactly through Caco-2 cell monolayers via a paracellular pathway (Ding et al., 2014). Peptide QAGLSPVR (IC_{50}=68.35 μmol/L), which has proven clear ACE inhibitory potency in vitro and on spontaneously hypertensive rats, can transport through the Caco-2 cell monolayer via the paracellular pathway (Sun et al., 2019). However, two corn gluten-derived peptides YFCLT and GLLLPH transport across Caco-2 cell monolayers via both energy-dependent transcytosis and the paracellular pathway (Ding et al., 2018). A long-residue peptide (YQEPALGPVRGPFPIIV) from milk can transport through the Caco-2 cell monolayer involved in transcytosis transport (Regazzo et al., 2010). So peptides in our study might be absorded via transcytosis or the paracellular pathway.

5 Conclusions

Food-derived multi-target peptides could be used as resources to explore the inhibition mechanisms of ACE inhibitory peptides. We examined four black tea peptides all located in a cavity away from the active site pocket of ACE. The peptides in this study were identified from black tea without any treatment of exogenous enzymes. The stability and bioavailability of black tea peptides in vivo still require further investigation. We endeavoured to find more bioactive peptides from tea in many different ways. The ACE inhibitory peptides discovered from black tea have potential for antihypertension and will contribute to a new conception of black tea consumption.

Acknowledgments

The research was supported by the National Key Research and Development Program of China (No. 2016YFD0200900) and the Science Technology Department of Zhejiang Province (No. 2016C02053-8), China.

Author contributions

Yating LU performed the experimental research and data analysis, and wrote and edited the manuscript. Yu WANG, Danyi HUANG, and Dongmei FAN performed the data analysis. Zhuang BIAN performed the experimental research. Peng LU reviewed and edited the manuscript. Xiaochang WANG supervised the research, and reviewed and edited the manuscript. All authors have read and approved the final manuscript and, therefore, have full access to all the data in the study and take responsibility for the integrity and security of the data.

Compliance with ethics guidelines

Yating LU, Yu WANG, Danyi HUANG, Zhuang BIAN, Peng LU, Dongmei FAN, and Xiaochang WANG declare that they have no conflict of interest.

This article does not contain any studies with human or animal subjects performed by any of the authors.

References

Asoodeh A, Yazdi MM, Chamani J, 2012. Purification and characterisation of angiotensin I converting enzyme inhibitory peptides from lysozyme hydrolysates. *Food Chem*, 131(1):291-295. https://doi.org/10.1016/j.foodchem.2011.08.039

Bougatef A, Nedjar-Arroume N, Ravallec-Plé R, et al., 2008. Angiotensin I-converting enzyme (ACE) inhibitory activities of sardinelle (*Sardinella aurita*) by-products protein hydrolysates obtained by treatment with microbial and visceral fish serine proteases. *Food Chem*, 111(2):350-356. https://doi.org/10.1016/j.foodchem.2008.03.074

Case DA, Cheatham TE III, Darden T, et al., 2005. The amber biomolecular simulation programs. *J Computat Chem*, 26(16):1668-1688. https://doi.org/10.1002/jcc.20290

Chamata Y, Watson KA, Jauregi P, 2020. Whey-derived peptides interactions with ACE by molecular docking as a potential predictive tool of natural ACE inhibitors. *Int J Mol Sci*, 21(3):864. https://doi.org/10.3390/ijms21030864

Cheung BMY, Li C, 2012. Diabetes and hypertension: is there a common metabolic pathway? *Curr Atheroscler Rep*, 14(2):160-166. https://doi.org/10.1007/s11883-012-0227-2

Collier SR, Landram MJ, 2012. Treatment of prehypertension: lifestyle and/or medication. *Vasc Health Risk Manag*, 8:613-619. https://doi.org/10.2147/vhrm.S29138

Dang YL, Zhou TY, Hao L, et al., 2019. In vitro and in vivo studies on the angiotensin-converting enzyme inhibitory activity peptides isolated from broccoli protein hydrolysate. *J Agric Food Chem*, 67(24):6757-6764. https://doi.org/10.1021/acs.jafc.9b01137

Daskaya-Dikmen C, Yucetepe A, Karbancioglu-Guler F, et al., 2017. Angiotensin-I-converting enzyme (ACE)-inhibitory peptides from plants. *Nutrients*, 9(4):316. https://doi.org/10.3390/nu9040316

Ding L, Zhang Y, Jiang YQ, et al., 2014. Transport of egg white ACE-inhibitory peptide, Gln-Ile-Gly-Leu-Phe, in human intestinal Caco-2 cell monolayers with cytoprotective effect. *J Agric Food Chem*, 62(14):3177-3182. https://doi.org/10.1021/jf405639w

Ding L, Wang LY, Zhang T, et al., 2018. Hydrolysis and transepithelial transport of two corn gluten derived bioactive peptides in human Caco-2 cell monolayers. *Food Res Int*, 106:475-480. https://doi.org/10.1016/j.foodres.2017.12.080

Escudero E, Mora L, Fraser PD, et al., 2013. Purification and identification of antihypertensive peptides in Spanish dry-cured ham. *J Proteomics*, 78:499-507. https://doi.org/10.1016/j.jprot.2012.10.019

Ettehad D, Emdin CA, Kiran A, et al., 2016. Blood pressure lowering for prevention of cardiovascular disease and death: a systematic review and meta-analysis. *Lancet*, 387(10022):957-967. https://doi.org/10.1016/s0140-6736(15)01225-8

Fan HB, Wang JP, Liao W, et al., 2019. Identification and characterization of gastrointestinal-resistant angiotensin-converting enzyme inhibitory peptides from egg white proteins. *J Agric Food Chem*, 67(25):7147-7156. https://doi.org/10.1021/acs.jafc.9b01071

Ferreira SH, 1965. A bradykinin-potentiating factor (BPF) present in the venom of *Bothrops jararaca*. *Br J Pharmacol Chemother*, 24(1):163-169. https://doi.org/10.1111/j.1476-5381.1965.tb02091.x

Forghani B, Zarei M, Ebrahimpour A, et al., 2016. Purification and characterization of angiotensin converting enzyme-inhibitory peptides derived from *Stichopus horrens*: stability study against the ACE and inhibition kinetics. *J Funct Foods*, 20:276-290. https://doi.org/10.1016/j.jff.2015.10.025

García-Mora P, Martín-Martínez M, Angeles Bonache M, et al., 2017. Identification, functional gastrointestinal stability and molecular docking studies of lentil peptides with dual antioxidant and angiotensin I converting enzyme inhibitory activities. *Food Chem*, 221:464-472. https://doi.org/10.1016/j.foodchem.2016.10.087

Groneberg DA, Döring F, Eynott PR, et al., 2001. Intestinal peptide transport: ex vivo uptake studies and localization of peptide carrier PEPT1. *Am J Physiol-Gastrointestin Liver Physiol*, 281(3):G697-G704. https://doi.org/10.1152/ajpgi.2001.281.3.G697

Guan SS, Han WW, Zhang H, et al., 2016. Insight into the interactive residues between two domains of human somatic Angiotensin-converting enzyme and Angiotensin II by MM-PBSA calculation and steered molecular dynamics simulation. *J Biomol Struct Dyn*, 34(1):15-28. https://doi.org/10.1080/07391102.2015.1007167

Gu Y, Majumder K, Wu JP, 2011. QSAR-aided in silico approach in evaluation of food proteins as precursors of ACE inhibitory peptides. *Food Res Int*, 44(8):2465-2474. https://doi.org/10.1016/j.foodres.2011.01.051

Gunalan S, Somarathinam K, Bhattacharya J, et al., 2020. Understanding the dual mechanism of bioactive peptides targeting the enzymes involved in renin angiotensin system (RAS): an in-silico approach. *J Biomol Struct Dyn*, 38(7):5044-5061. https://doi.org/10.1080/07391102.2019.1695668

Hanif K, Bid HK, Konwar R, 2010. Reinventing the ACE inhibitors: some old and new implications of ACE inhibition. *Hypertens Res*, 33(1):11-21. https://doi.org/10.1038/hr.2009.184

Harrison C, Acharya KR, 2014. ACE for all—a molecular perspective. *J Cell Commun Signal*, 8(3):195-210. https://doi.org/10.1007/s12079-014-0236-8

Homeyer N, Gohlke H, 2012. Free energy calculations by the molecular mechanics poisson-boltzmann surface area method. *Mol Inform*, 31(2):114-122. https://doi.org/10.1002/minf.201100135

Kumar R, Chaudhary K, Chauhan JS, et al., 2015. An in silico platform for predicting, screening and designing of anti-hypertensive peptides. *Sci Rep*, 5: 12512. https://doi.org/10.1038/srep12512

Lacroix IME, Meng GT, Cheung IWY, et al., 2016. Do whey protein-derived peptides have dual dipeptidyl-peptidase IV and angiotensin I-converting enzyme inhibitory activities? *J Funct Foods*, 21:87-96. https://doi.org/10.1016/j.jff.2015.11.038

Lafarga T, Hayes M, 2017. Bioactive protein hydrolysates in the functional food ingredient industry: overcoming current challenges. *Food Rev Int*, 33(3):217-246. https://doi.org/10.1080/87559129.2016.1175013

Laskowski RA, Swindells MB, 2011. LigPlot+: multiple ligand-protein interaction diagrams for drug discovery. *J Chem Inf Model*, 51(10):2778-2786. https://doi.org/10.1021/ci200227u

Li DX, Wang RR, Huang JB, et al., 2019. Effects and mechanisms of tea regulating blood pressure: evidences and promises. *Nutrients*, 11(5):1115. https://doi.org/10.3390/nu11051115

Li Y, Sadiq FA, Liu TJ, et al., 2015. Purification and identification of novel peptides with inhibitory effect against angiotensin I-converting enzyme and optimization of process conditions in milk fermented with the yeast *Kluyveromyces marxianus*. *J Funct Foods*, 16:278-288. https://doi.org/10.1016/j.jff.2015.04.043

Liu C, Fang L, Min W, et al., 2018. Exploration of the molecular interactions between angiotensin-I-converting enzyme (ACE) and the inhibitory peptides derived from hazelnut (*Corylus heterophylla* Fisch.). *Food Chem*, 245:471-480. https://doi.org/10.1016/j.foodchem.2017.10.095

Lu YT, Lu P, Wang Y, et al., 2019. A novel dipeptidyl peptidase IV inhibitory tea peptide improves pancreatic β-cell function and reduces α-cell proliferation in streptozotocin-induced diabetic mice. *Int J Mol Sci*, 20(2):322. https://doi.org/10.3390/ijms20020322

Majumder K, Chakrabarti S, Morton JS, et al., 2015. Egg-derived ACE-inhibitory peptides IQW and LKP reduce blood pressure in spontaneously hypertensive rats. *J Funct Foods*, 13:50-60. https://doi.org/10.1016/j.jff.2014.12.028

Martin M, Deussen A, 2019. Effects of natural peptides from food proteins on angiotensin converting enzyme activity and hypertension. *Crit Rev Food Sci Nutr*, 59(8):1264-1283. https://doi.org/10.1080/10408398.2017.1402750

Mills KT, Bundy JD, Kelly TN, et al., 2016. Global disparities of hypertension prevalence and control: a systematic analysis of population-based studies from 90 countries. *Circulation*, 134(6):441-450. https://doi.org/10.1161/circulationaha.115.018912

Miner-Williams WM, Stevens BR, Moughan PJ, 2014. Are intact peptides absorbed from the healthy gut in the adult human? *Nutr Res Rev*, 27(2):308-329. https://doi.org/10.1017/s0954422414000225

Minkiewicz P, Dziuba J, Iwaniak A, et al., 2008. Biopep database and other programs for processing bioactive peptide sequences. *J AOAC Int*, 91(4):965-980. https://doi.org/10.1093/jaoac/91.4.965

Ning XY, Zhang YL, Yuan TT, et al., 2018. Enhanced thermostability of glucose oxidase through computer-aided molecular design. *Int J Mol Sci*, 19(2):425. https://doi.org/10.3390/ijms19020425

Patil P, Mandal S, Tomar SK, et al., 2015. Food protein-derived bioactive peptides in management of type 2 diabetes. *Eur J Nutr*, 54(6):863-880. https://doi.org/10.1007/s00394-015-0974-2

Puchalska P, Marina Alegre ML, García López MC, 2015. Isolation and characterization of peptides with antihypertensive activity in foodstuffs. *Crit Rev Food Sci Nutr*, 55(4):521-551. https://doi.org/10.1080/10408398.2012.664829

Regazzo D, Mollé D, Gabai G, et al., 2010. The (193–209) 17-residues peptide of bovine β-casein is transported through Caco-2 monolayer. *Mol Nutr Food Res*, 54(10): 1428-1435. https://doi.org/10.1002/mnfr.200900443

Saito Y, Wanezaki K, Kawato A, et al., 1994. Structure and activity of angiotensin I converting enzyme inhibitory peptides from sake and sake lees. *Biosci Biotechnol Biochem*, 58(10):1767-1771. https://doi.org/10.1271/bbb.58.1767

Satoh E, Tohyama N, Nishimura M, 2005. Comparison of the antioxidant activity of roasted tea with green, oolong, and black teas. *Int J Food Sci Nutr*, 56(8):551-559. https://doi.org/10.1080/09637480500398835

Shalaby SM, Zakora M, Otte J, 2006. Performance of two commonly used angiotensin-converting enzyme inhibition assays using FA-PGG and HHL as substrates. *J Dairy Res*, 73(2):178-186. https://doi.org/10.1017/s0022029905001639

Sharma A, Singla D, Rashid M, et al., 2014. Designing of peptides with desired half-life in intestine-like environment. *BMC Bioinformatics*, 15:282. https://doi.org/10.1186/1471-2105-15-282

Shen YM, Maupetit J, Derreumaux P, et al., 2014. Improved PEP-FOLD approach for peptide and miniprotein structure prediction. *J Chem Theory Comput*, 10(10):4745-4758. https://doi.org/10.1021/ct500592m

Shimizu M, 1999. Modulation of intestinal functions by food substances. *Nahrung*, 43(3):154-158. https://doi. org/10.1002/(SICI)1521-3803(19990601)43: 3 <154::AID-FOOD154>3.0.CO;2-A

Sornwatana T, Bangphoomi K, Roytrakul S, et al., 2015. Chebulin: *Terminalia chebula* Retz. fruit-derived peptide with angiotensin-I-converting enzyme inhibitory activity. *Biotechnol Appl Biochem*, 62(6):746-753. https://doi.org/10.1002/bab.1321

Sun LP, Wu BY, Yan MY, et al., 2019. Antihypertensive effect in vivo of QAGLSPVR and its transepithelial transport through the Caco-2 cell monolayer. *Mar Drugs*, 17(5):288. https://doi.org/10.3390/md17050288

Tanzadehpanah H, Asoodeh A, Saberi MR, et al., 2013. Identification of a novel angiotensin-I converting enzyme inhibitory peptide from ostrich egg white and studying its interactions with the enzyme. *Innovat Food Sci Emerg Technol*, 18:212-219. https://doi.org/10.1016/j.ifset.2013.02.002

Tao C, Yu DH, Cornelius V, et al., 2017. Potential health impact and cost-effectiveness of drug therapy for prehypertension. *Int J Cardiol*, 240:403-408. https://doi.org/10.1016/j.ijcard.2017.05.003

Tao ML, Sun HJ, Liu L, et al., 2017. Graphitized porous carbon for rapid screening of angiotensin-converting enzyme inhibitory peptide GAMVVH from silkworm pupa protein and molecular insight into inhibition mechanism. *J Agric Food Chem*, 65(39):8626-8633. https://doi.org/10.1021/acs.jafc.7b03195

Trott O, Olson AJ, 2010. AutoDock Vina: improving the speed and accuracy of docking with a new scoring function, efficient optimization, and multithreading. *J Comput Chem*, 31(2):455-461. https://doi.org/10.1002/jcc.21334

Wang Q, Wang Y, Chen GJ, 2016. Influence of secondary-structure folding on the mutually exclusive folding process of GL5/I27 protein: evidence from molecular dynamics simulations. *Int J Mol Sci*, 17(11):1962. https://doi.org/10.3390/ijms17111962

Wang YF, Yang ZW, Wei XL, 2010. Sugar compositions, α-glucosidase inhibitory and amylase inhibitory activities of polysaccharides from leaves and flowers of *Camellia sinensis* obtained by different extraction methods. *Int J Biol Macromol*, 47(4):534-539. https://doi.org/10.1016/j.ijbiomac.2010.07.007

Wu QY, Jia JQ, Yan H, et al., 2015. A novel angiotensin-I converting enzyme (ACE) inhibitory peptide from gastrointestinal protease hydrolysate of silkworm pupa (*Bombyx mori*) protein: biochemical characterization and molecular docking study. *Peptides*, 68:17-24. https://doi.org/10.1016/j.peptides.2014.07.026

Yu DY, Wang C, Song YF, et al., 2019. Discovery of novel angiotensin-converting enzyme inhibitory peptides from *Todarodes pacificus* and their inhibitory mechanism: in silico and in vitro studies. *Int J Mol Sci*, 20(17):4159. https://doi.org/10.3390/ijms20174159

Zhang ZF, Li Q, Liang J, et al., 2010. Epigallocatechin-3-*O*-gallate (EGCG) protects the insulin sensitivity in rat L6 muscle cells exposed to dexamethasone condition. *Phytomedicine*, 17(1):14-18. https://doi.org/10.1016/j.phymed.2009.09.007

Zhao TR, Liu BT, Yuan L, et al., 2019. ACE inhibitory activity in vitro and antihypertensive effect in vivo of LSGYGP and its transepithelial transport by Caco-2 cell monolayer. *J Funct Foods*, 61:103488. https://doi.org/10.1016/j.jff.2019.103488

Zheng YJ, Wang X, Zhuang YL, et al., 2019. Isolation of novel ACE-inhibitory and antioxidant peptides from quinoa bran albumin assisted with an in silico approach: characterization, in vivo antihypertension, and molecular docking. *Molecules*, 24(24):4562. https://doi.org/10.3390/molecules24244562

Zheng YJ, Wang X, Zhuang YL, et al., 2020. Isolation of novel ACE-inhibitory peptide from naked oat globulin hydrolysates in silico approach: molecular docking, in vivo antihypertension and effects on renin and intracellular endothelin-1. *J Food Sci*, 85(4):1328-1337. https://doi.org/10.1111/1750-3841.15115